

# Dynamic motion of lean swirling premixed flame generated by change in gravitational orientation

H. Gotoda<sup>\*1</sup>, T. Miyano<sup>2</sup>, I.G. Shepherd<sup>3</sup>

<sup>1</sup> Department of Mechanical Engineering, Ritsumeikan University,  
1-1-1 Nojihigashi, Kusatsu, Shiga 525-8577, Japan

<sup>2</sup> Department of Micro System Technology, Ritsumeikan University,  
1-1-1 Nojihigashi, Kusatsu, Shiga 525-8577, Japan

<sup>3</sup> Combustion Group, Advanced Energy Technologies Department, Environmental Energy Technologies Division,  
Lawrence Berkeley National Laboratory, Berkeley, California 94720, USA

## Abstract

The dynamic behavior of swirling premixed flames generated by the effect of gravitational orientation has been experimentally investigated. When the gravitational direction relative to the flame front is changed, i.e., in inverted gravity (-1G), an unstably fluctuating flame (unstable flame) is formed in a limited domain of equivalence ratio and swirl number. The time history of the flame front fluctuation shows that high-energy chaotic motion superimposes on a periodical oscillation that is induced by buoyancy. This results in the dynamic motion of the unstable flame becoming deterministically chaotic. This is demonstrated by nonlinear time series analysis which has not been widely applied to the investigation of combustion phenomena.

## Introduction

The effect of buoyancy on generation and growth of flame instability issue has been one of main subjects of present day combustion science. There are two major instabilities generated by upward buoyant force (i.e., normal gravity (+1G): a) hydrodynamic shear layer instability associated with Kelvin-Helmholtz instability and b) Rayleigh-Taylor instability. In open premixed flames, the entire flow field consists predominantly of cold dense reactants (heavy gas) in upstream flow, hot combustion products (light gas) in downstream flow, and cold surrounding air (heavy gas). When the hot combustion products accelerated by the upward buoyant force interact with the cold surrounding air, the interface between these fluids becomes unstable owing to the hydrodynamic shear layer instability, resulting in a large-scale toroidal vortex at the interface. This vortex produces periodic velocity fluctuations in reactant flow and causes the flame front to oscillate at a distinct characteristic frequency (10~20Hz) [1-4]. In contrast, when one considers the +1G gravitational direction relative to the flame front, the interface between hot combustion products above cold dense reactants is stable for flow perturbations, while in the inverted gravity (-1G) case, the interface is unstable owing to Rayleigh-Taylor instability. By inverting the orientation of a burner system relative to the gravitational direction, light combustion products are formed below heavy reactants, and upward propagating flames become sensitive to the dynamic motion of the light combustion products. In fact, for lean premixed flames under low Reynolds number conditions, the overall flame configuration in -1G is significantly distorted [5], [6].

It is well known that swirling flow is one of the most important flow configurations for fundamental

combustion systems. Therefore, there is a need to understand how the buoyancy/swirl interaction affects flame front dynamics by changing the gravitational direction relative to the flame front. With respect to experimental investigations of the flame dynamics generated by swirling flow, the rotating burner that spins on its central axis is one of the most fundamental flame configurations [7]. In our preliminary work using a rotating Bunsen burner [8], we observed that changes in buoyancy/swirl interaction generated by the effect of the gravitational orientation may cause irregular fluctuations in flame front dynamics that are thought to be chaotic not turbulent. An investigation of the dynamical behavior of this flame instability by sophisticated nonlinear chaos analysis is important for gaining a comprehensive understanding of the complex nonlinear phenomena in flame dynamics.

The objective of this study is to conduct an experimental investigation of the dynamic behavior of the flame front generated by the inversion of the gravitational direction under the swirling flow conditions produced by a rotating Bunsen burner.

## Experimental details

The rotating Bunsen burner we used in this study is shown schematically in Fig. 1. The premixed CH<sub>4</sub>/air reactants flow through a diffuser, fine damping screens, a nozzle, and a straight burner tube. The burner tube has a diameter of 12 mm and is fitted on top of the nozzle, which is vertically supported by two bearings and rotated by a DC motor through a pulley and belt system. A 15 mm thick honeycomb section with a grid diameter of 1.04 mm is fitted inside the burner tube to produce the solid-body rotation of the reactants at the burner tube exit. The bulk flow velocity of the reactants

---

\* Corresponding author: gotoda@se.ritsumei.ac.jp

$U_0$  was varied from 1.0 m/s (buoyancy-dominated region:  $R_i > 0.1$ ) to 2.0 m/s (momentum-dominated region:  $R_i < 0.1$ ). The Richardson number  $R_i$  defined as  $((T_{ad} - T_0)/T_{ad})(GD_0/U_0^2)$ , where  $T_{ad}$  is the adiabatic flame temperature,  $T_0$  is the temperature of surrounding air,  $G$  is the gravitational acceleration, and  $D_0$  is the diameter of the straight tube, can be used to delineate flow conditions where buoyancy is significant,  $R_i < 0.1$ , and from those where it is not,  $R_i > 0.1$  [4], [5]. The Reynolds number  $Re$  based on the burner exit diameter is between 780 and 1560. The equivalence ratio of premixed reactants  $\phi$  was varied from 0.60 to 0.90. The rotational speed of the burner tube  $N$  was varied from 0 to 4500 rpm ( $75 \text{ s}^{-1}$ ). To characterize the balance between the axial momentum and the swirl momentum, the Swirl number  $S$  is introduced and was varied from 0 to 0.7.

To investigate the dynamical motion of the flame front, a laser tomographic method is used. The light source is an  $\text{Ar}^+$  laser (Lexel Model 95) with a maximum power of 2 W. Silicon oil droplets with diameters of 1~2  $\mu\text{m}$  are dispersed in reactants as scatters. The Mie scattered light emitted from the droplets shows the region where the temperature is below 570 K. The upstream side of the preheat zone can then be visualized by observing the front of the silicon oil droplets. The visualized images are recorded by a high-speed video camera (Photron 1024 PCI) of 1000 frames per second with a frame size of  $1024 \times 1024$  pixels. The spatial resolution of the images is 27 pixels per millimeter. As shown in Fig. 2, the location of the vaporized front along the centerline of the burner tube is defined as the flame front location  $y_f$  (mm) and the deviation from the mean flame front location  $\Delta y_f = y_f - \bar{y}_f$ . Here,  $\bar{y}_f$  is the time-averaged flame front location as a function of time  $t$  and is measured to investigate the dynamic motion of the unstable flame.

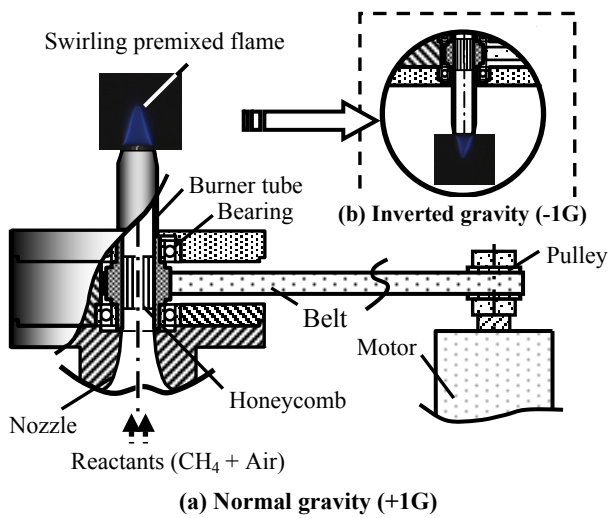


Figure 1 Experimental apparatus

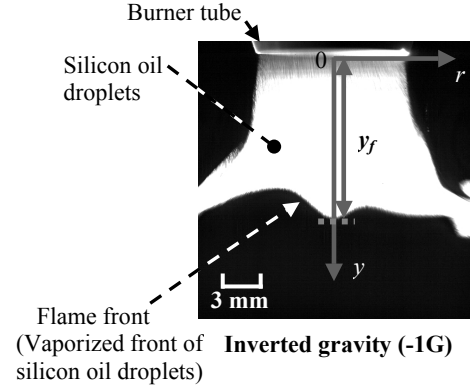


Figure 2 Definition of flame front location

### Nonlinear time series analysis

We briefly describe the central ideas behind the mathematics of each method of the time series analysis employed in this work.

On the basis of Taken's embedding theorem [9], the attractor is constructed from the time series of the deviation from the mean flame front location  $\Delta y_f$ . The time-delayed coordinates for the construction of the attractor are expressed as

$$\mathbf{X}(t) = (\Delta y_f(t), \Delta y_f(t - \tau_0), \dots, \Delta y_f(t - (D-1)\tau_0))$$

where  $i = 0, 1, \dots, n$  ( $n$  is the data number of the time series),  $\mathbf{X}_i$  are the constructed phase space vectors,  $\Delta y_f(t_i)$  is the deviation from mean flame front location at time  $t_i$ ,  $D$  is the embedding dimension, that is, the dimension of the constructed phase space and  $\tau_0$  is the suitable time lag. In this work,  $\tau_0$  is set to be either the time lag that yields a local minimum of mutual information, according to the prescription of Fraser and Swinney [10].

The diversity in the directions of neighboring trajectories in the constructed phase space is related to the degree of visible determinism in the dynamic behavior. On the basis of this fact, we use the algorithm that was proposed by Wayland et al. in order to test for determinism in a time series [12]. Let us randomly select a vector  $\mathbf{X}(t_0)$  and find its  $K$  nearest neighbors  $\mathbf{X}(t_k)$  with  $k$  from 1 to  $K$ . We may set the images of all the vectors to  $\mathbf{X}(t_k + \tau_0)$  with  $k$  from 0 to  $K$ . The diversity in the directions of nearby trajectories is measured in terms of the translation error  $E_{trans}$  defined by

$$E_{trans} = \frac{1}{K+1} \sum_{k=0}^K \frac{\|\mathbf{V}(t_k) - \bar{\mathbf{V}}\|^2}{\|\bar{\mathbf{V}}\|^2}$$

$$\bar{\mathbf{V}} = \frac{1}{K+1} \sum_{k=0}^K \mathbf{V}(t_k)$$

$$\mathbf{V}(t_k) = \|\mathbf{X}(t_k + \tau_0) - \mathbf{X}(t_k)\|$$

Here,  $\mathbf{V}(t_k)$  approximates the tangential vectors of the trajectories at time  $t_k$ . The more parallel the trajectories are to each other, that is, the more visible determinism there is in the time series, the closer  $E_{trans}$  will be to zero. In a previous numerical work, it was shown that a time

series can be regarded as a deterministic (chaos) process if  $E_{trans} < 0.5$  and as a stochastic process if  $E_{trans} > 0.5$ . In the case of white noise,  $E_{trans} \approx 1$  independent of the embedding dimension.

## Results and Discussion

Changes in the overall flame shapes of swirling flames in the buoyancy-dominated region ( $U_0 = 1.0$  m/s,  $Re = 780$ ,  $R_i \approx 0.1$ ) are shown in Fig. 3 as functions of the equivalence ratio  $\phi$  and swirl number  $S$  in normal gravity (+1G) and inverted gravity (-1G). The lines represent the transition boundary between the flame shapes. In the case of normal gravity, as  $S$  increases under  $\phi > 0.8$ , the flame shape changes from a conical shape to a skewed (eccentric) shape with the flame tips whirling around the rotational axis of the burner tube. This is due to the deviation of the flame tip from the centerline of the burner tube generated by the centrifugal force on initial reactants. As the degree of deviation increases with increasing  $S$ , it becomes more skewed shape (tilted shape) with portions of the flame moving inside the burner tube. At leaner equivalence ratios with  $\phi < 0.75$ , the flame base is lifted above the burner tube exit and a flat flame is formed.

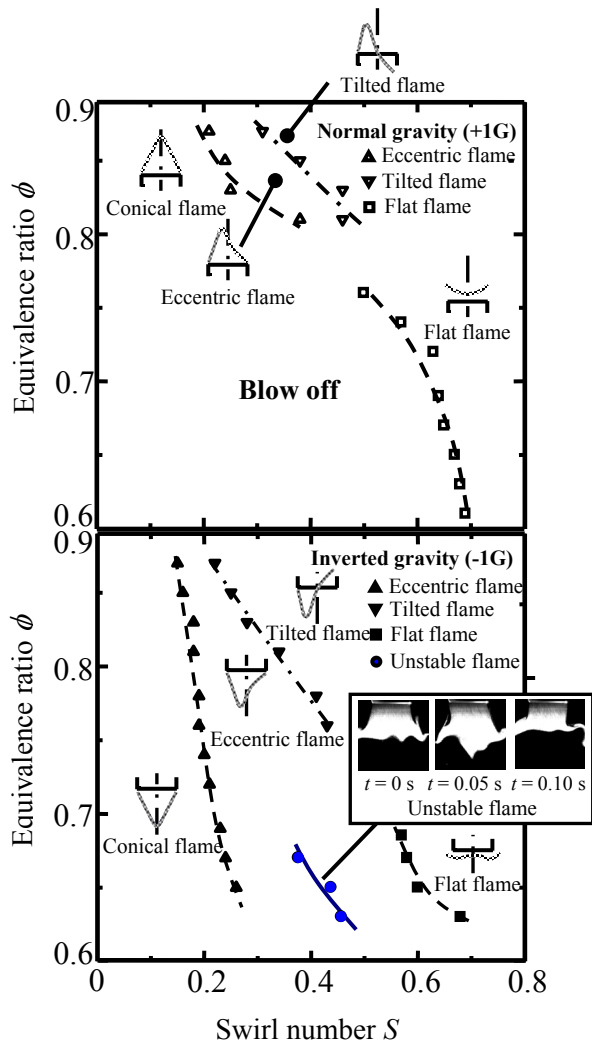


Figure 3 Flame shape variation as function of equivalence ratio and swirl number

In contrast to the +1G case, when the orientation of the burner system relative to the gravitational direction is changed, i.e., in inverted gravity (-1G), the transition boundary between these flame shapes changes considerably and shifts to a lower Swirl number. These results indicate that the change in gravitational orientation relative to the flame front has a significant impact on the overall flame shapes of swirling flames. The most interesting phenomenon generated by the inversion of the gravitational orientation is the formation of an unstable flame with its front switching back and forth between a stable eccentric and a stable flat flame. As shown in the time sequence images (in the inset in Fig. 3) obtained by laser tomographic method, the flame front of this unstable flame fluctuates with a large deformation of the flame front configuration.

For two representative cases of unstable flames observed in the buoyancy-dominated ( $U_0 = 1.0$  m/s,  $Re = 780$ ,  $R_i \approx 0.1$ ) and momentum dominated regions ( $U_0 = 1.8$  m/s,  $Re = 1403$ ,  $R_i \approx 0.03$ ), the deviation from the mean value of the flame front location  $\Delta y_f$  as a function of time  $t$  and the power spectrum obtained by fast Fourier transform (FFT) analysis are shown in Fig. 4. As depicted in the inset in Fig. 4,  $\Delta y_f$  at  $U_0 = 1.0$  m/s fluctuates irregularly with time. However, the power spectrum does not exhibit only a broad-band structure. In fact, it exhibits a peak at approximately 10.3 Hz, indicating a periodic oscillation. This is nearly the same as that caused by the buoyancy-induced hydrodynamic shear layer instability in normal gravity [4]. This frequency cannot normally be formed in the inverted gravity case because the onset of the buoyancy-induced large-scale toroidal vortex at the interface between combustion products and surrounding air is suppressed [4], [5]. However, the result obtained by FFT analysis indicates that under a specified condition in inverted gravity, the hydrodynamic instability associated with an upward buoyant force probably may be related to the onset of the dominant oscillation mode of the unstable flame. In addition to this oscillation frequency, many small peaks also appear in the power spectrum. These peaks make the dynamic behavior of  $\Delta y_f$  complex. The fluctuation of  $\Delta y_f$  becomes more complex and the spectrum has a higher frequency tail at  $U_0 = 1.8$  m/s than at  $U_0 = 1.0$  m/s. The power density of the oscillation frequency corresponding to that of the dominant oscillation observed at  $U_0 = 1.0$  m/s apparently decreases to the same level as some small peaks. This indicates that the periodic oscillation, possibly as a result of the hydrodynamic instability associated with buoyancy, can survive in flame dynamics even in momentum-dominated regions. The significant change in entire power spectrum distribution can be attributed to the hydrodynamic fluctuations of initial reactants in itself due to increases in axial and radial flow momentum.

The translation error  $E_{trans}$  was estimated as a function of embedding dimension  $D$ , as shown in Fig. 5. At  $U_0 = 1.0$  m/s,  $E_{tran}$  significantly decreases with increasing  $D$  and becomes constant when  $D$  exceeds 8.

The crossing of neighboring trajectories in phase space is minimal at  $D \geq 8$ , resulting in an observable determinism similar to a finite-dimensional chaos. Although the saturated values of  $E_{trans}$  are slightly larger than the criterion value ( $E_{trans} = 0.1$ ) below which determinism can be said to be observable, they are lower than those of temporally correlated random fluctuations representing stochastic processes ( $E_{trans} > 0.5$ ). These results suggest that the dynamic behavior of the unstable flame observed at  $U_0 = 1.0$  m/s represents a deterministic chaos. With  $U_0$  increasing up to 1.8 m/s,  $E_{trans}$  saturates at  $D \geq 10$  and increases up to approximately 0.22, possibly indicating a high-dimensional chaos. The dynamic behavior of the unstable flame can be considered a deterministic chaos even in momentum-dominated regions. The deterministic nature of the flame dynamics will become invisible if the flame front motion becomes turbulent with further increases in the axial and radial flow momentum of reactants. These results show that we can clarify the characteristics of complex flame instability by nonlinear time series analysis. As explained, the result of FFT analysis shows that a periodic oscillation mode dominates the dynamic behavior of the unstable flame in the buoyancy-dominated region. On the basis of this result, the chaotic irregular fluctuation included in the time series data is superimposed on the dominant periodic oscillation, resulting in a complex motion of the flame front dynamics under buoyancy-dominated conditions.

### Summary

The dynamic behavior of the swirling premixed flame generated by the effect of gravitational orientation has been experimentally and numerically investigated under flow conditions that span the buoyancy-dominated ( $R_i > 0.1$ ) and momentum-dominated ( $R_i < 0.1$ ) regimes. When the gravitational direction is changed relative to the flame front, i.e., in inverted gravity (-1G), interestingly, an unstably fluctuating flame (unstable flame) is formed between a stable eccentric flame and a stable flat flame in a limited domain of equivalence ratio and swirl number. Under buoyancy-dominated conditions, the chaotic irregular fluctuation included in the flame front motion is superimposed on the periodical oscillation of the unstable flame. As a result, the dynamic behavior of the unstable flame becomes a deterministic chaos. Its dynamics progressively develops into a high-dimensional chaos under momentum-dominated conditions. This result was demonstrated by the use of nonlinear time series analysis which has not been widely applied to the investigation of combustion phenomena. The analytical methods we applied in this work were shown to be valid for quantifying the complex flame instability characteristics of a lean swirling premixed flame.

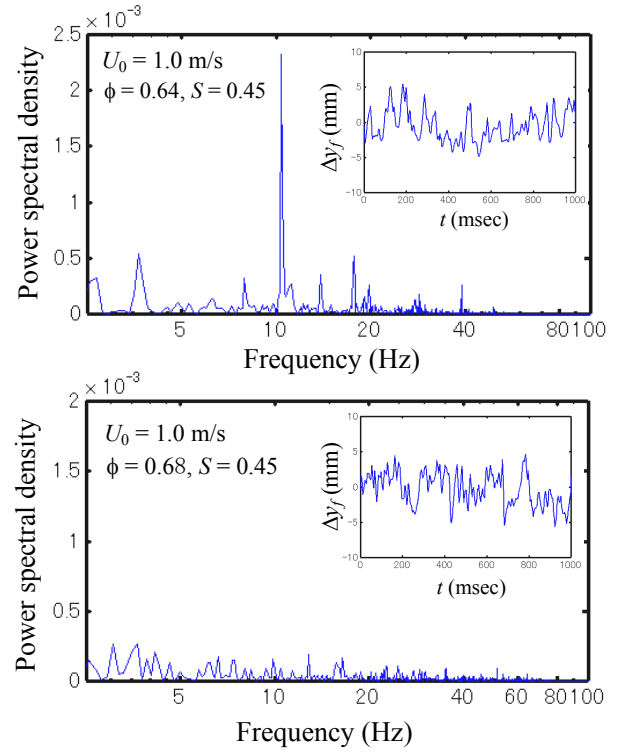


Figure 4 Power spectrum of unstable flame motion

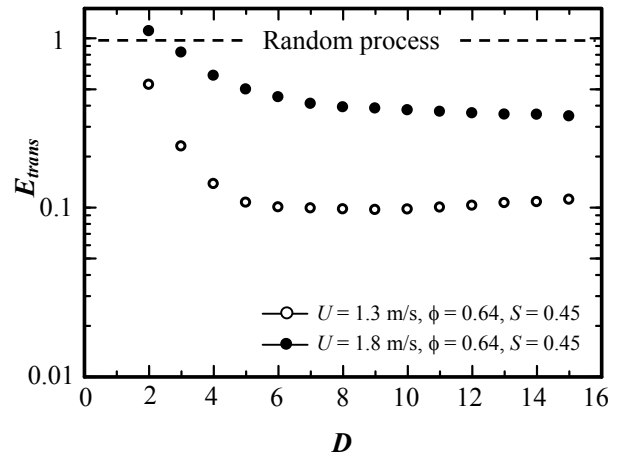


Figure 5 Translation error as function of embedding dimension

### Acknowledgement

Two of the authors (HG and TM) are supported by a “Research Grant from The Mazda Foundation”, “Research Grant from Kurata Hitachi Science Technology Foundation”, “the CASIO Science Foundation” and a “Grant-in-Aid for Young Scientists (B) from the Ministry of Education, Culture, Sports, Science and Technology of Japan (MEXT)”. The work is also supported (IGS) by the NASA Microgravity Program through the US Department of Energy under Contact No. DE-AC02-05CH11231 and monitored by Dr. Paul Greenberg.

## References

- [1] D. Durox, F. Baillot, R. Scoufflaire, and Prudhomme, *Combust. Flame* 82 (1990) 66.
- [2] D. Durox, T. Yuan, F. Baillot, and J. M. Most, *Combust. Flame* 102 (1995) 501.
- [3] L. W. Kostiuk and R. K. Cheng, *Exp. Fluids* 18 (1994) 59.
- [4] L. W. Kostiuk and R. K. Cheng, *Combust. Flame* 103 (1995) 27.
- [5] B. Bedat and R. K. Cheng, *Combust. Flame* 107 (1996) 13.
- [6] R. K. Cheng, B. Bedat, and L. W. Kostiuk, *Combust. Flame* 116 (1999) 360.
- [7] H. Gotoda and T. Ueda, *Combust. Flame* 140 (2005) 287.
- [8] H. Gotoda and I. G. Shepherd, 21th International Colloquium on the Dynamics of Explosions and Reactive Systems, France (2007).
- [9] F. Takens, *Lecture Notes in Mathematics*, 898 Springer, New York (1981) 366.
- [10] A. M. Fraser and H. L. Swinney, *Phys. Rev. A* 3 (1986) 1134.
- [11] P. Grassberger and I. Procaccia, *Phys. Rev. Lett.* 31 (1983) 346.
- [12] R. Wayland, D. Bromley, D. Pickett, and A. Passamante, *Phys. Rev. Lett.* 70 (1993) 580.